



Vibration Analysis as Useful Domain for detection of Bearing Fault Signals in Induction Motors

M. Tabasi, M. Ojaghi*, M. Mostafavi

Department of Electrical Engineering, University of Zanjan, Zanjan, Iran

PAPER INFO

Paper history:

Received 2 Desember 2020

Received in revised form 08 June 2021

Accepted 23 June 2021

Keywords:

Induction Motor

Bearing Fault

Fault Detection

Vibration Analysis

Vibration Signal

ABSTRACT

Due to widespread usage of induction motor (IM) in various industries, the requirement for its condition monitoring have been considerably raised. It is essential to detect faults that happened in IMs in a short time with high accuracy because they may cause considerable financial losses. Bearing faults contribute to a large percentage of IM failures. In this paper, vibration signal is analyzed for getting reliable indicator for faulty modes of the bearings of the IMs. The proper direction for measuring the vibration signal is analyzed first. This analysis showed that the fault-related vibration frequency components along the Z-axis, i.e. the axis perpendicular to the motor's installing surface, usually have the largest magnitude. Thus, it is recommended to measure the vibration signal in the Z-axis. Then, the bearing fault diagnosis using the vibration signal is investigated in various scenarios. The results confirm that the vibration indicators are not sensitive to environmental parameters like temperature and also load variation of the IM but the severity of the fault has a considerable influence on them.

doi: 10.5829/ije.2021.34.08b.22

NOMENCLATURE

f_{IR}	The vibration characteristic frequencies for the defect in the inner race	φ	Ball contact angle
f_{OR}	The vibration characteristic frequencies for the defect in the outer race	D_c	Mean diameter of the bearing
f_{CF}	The vibration characteristic frequencies for the defect in the cage	D_1	Inner diameter of the outer race
f_{BF}	The vibration characteristic frequencies for the defect in the balls	D_2	Outer diameter of the inner race
f_r	shaft rotational speed	D_b	Diameter of the balls
N_b	number of balls		

1. INTRODUCTION

Today, the trend towards induction machines (IMs), especially in the industry, is growing due to its simple configuration and high reliability. Although induction machines are very reliable, but they may encounter a variety of mechanical or electrical defects. The defects may either stem from the operation or exist inherently and they cause financial losses [1]. Therefore, condition monitoring and fault detection of IMs is a major issue and hence recently, a lot of researches are conducted in this regard. Some research showed that about 41 percent of total failures of induction motors are due to their bearing faults [2]. The bearing fault may occur in the manufacturing process or operation of the IM and it is

vital to detect quickly and accurately. The bearing faults may be detected by acoustic measurements, vibration measurements, temperature measurements, wear debris analysis, etc. [3-4].

Vibration measurement and analysis is the oldest method which can detect not only mechanical but also electrical faults with high accuracy. Different faults usually cause vibration with different frequencies in the IM. Therefore, the faults are detected by determining major frequencies of the vibration signal using spectrum analysis. However, while the vibration analysis brings numerous advantages, it requires installation measuring transducers on the motor body. Moreover, some resonant frequencies may affect the main vibration signal [5].

*Corresponding Author Institutional Email: mojaghi@znu.ac.ir (M. Ojaghi)

Spectral analysis is used in order to analyze the vibration through its characteristic frequencies [6]. The vibration is a complex motion and it is analyzed by spectral modulation to detect the bearing failures [7]. In other words, IM failures like bearing fault can be investigated by analyzing special characteristic frequencies in its vibration signal [8]. Thus, this method can be considered as an accurate and fast approach for the fault detection. The vibration analysis is examined as an efficient method for diagnosing electromagnetic problems in induction motors [9, 10]. Also, in order to perfectly predict mechanical faults, it was confirmed by Gangsar and Tiwari [11] that the analysis of the vibration signal is an efficient method and there is no need to analyze the electrical current signal.

Many studies have confirmed the role of vibration analysis in fault detection of induction motor. A vibration detection system is designed by Kuspiani et al. [12] that can be used for online monitoring of an induction motor. Induction motor vibration data is read from two vibration sensors and the results are analyzed by using artificial intelligence-based analysis. The partially damaged rotor bar under load changes using wavelet transform analysis is investigated by Rangel-Magdaleno et al. [13] and the required features are extracted from the vibration signals at different levels of failure. A squirrel cage induction motor is selected to predict its sound based on the results obtained through FFT analysis [14]. In this paper, the FFT results are compared with ISO standard vibration charts in order to consider preventative condition. Two diagnosis techniques are presented which are based on the stator current and the vibration using FFT [15]. The result of vibration analysis was as accurate as that of current analysis. A novel method entitled EMD-FFT was proposed by Moiz et al. [16] for vibration analysis of an IM. According to this method, the signal is decomposed into its intrinsic mode functions (IMFs) and then each IMF is analyzed by FFT. In addition, a comparison between the current and vibration based techniques is performed for the bearing fault detection and analysis [17].

Induction motor fault detection is investigated on the basis of the acoustic sound and vibration signals by Delgado-Arredondo et al. [18]. On that work, a method that is called the Complete Ensemble Empirical Mode Decomposition is used for decomposing the signal. Spectral analysis was proposed by Novoa et al. [19] for various frequencies in the motor vibration by using of Compact RIO equipment, LabVIEW, triaxle accelerometers, and low-pass filters. Moreover, a simulation system for unbalanced loading condition of a three-phase induction motor was proposed by Salah et al. [20]. An experimental study has been presented by Marignetti et al. [21] that focused on the vibration as well as acoustic noise emitted by the inverter-fed induction

motor. In this paper, a control technique based on the SVPWM is performed for using vibration and acoustic noise experimental analysis in order to control the phase voltages of a three-phase induction motor. Despite previous methods that were based on the detection of bearing fault occurrence, the time and frequency features of construct regression models were extracted for predicting the bearing faults [22].

In this paper, the aim is to investigate vibration domain for the bearing fault detection in the IMs through comprehensive laboratory test results. As shown in Figure 1, the vibration signal may be measured along with three perpendicular axes that are the X-, Y- and Z-axes. The vibration signals experimentally sampled in the three axes are first evaluated using frequency spectrum analysis to identify the most reliable direction for the vibration measurement aiming the bearing fault detection. The evaluation showed that the Z-axis, i.e. the axis perpendicular to the motor's installing surface, is the most reliable direction for this purpose. Then, the vibration signals measured in the Z-axis are used for analyzing the bearing fault-related frequency components to determine their sensitivity to the different bearing faults intensities as well as the load torque change and the temperature rise. According to the investigation results, the vibration frequency components are sensitive enough to detect and discriminate different bearing faults, while they are almost insensitive to the temperature rise and load torque change. Therefore, the main contribution and advantages achieved by this paper are as follows:

- Collecting and analyzing comprehensive experimental vibration test results in the three axes under different bearing fault types and severities, load torques and temperatures.
- Using the test results to determine the most reliable direction for measuring the vibration signal aiming the bearing fault detection.
- Using the test results to determine the sensitivity of the vibration frequency components to detect different bearing fault types.
- Using the test results to determine the most insensitive vibration frequency components to the load torque and temperature rise.

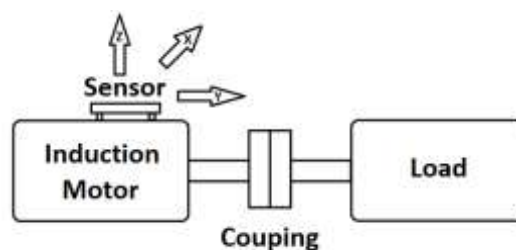


Figure 1. Three different directions on IM

The paper organization is as follows: Section 2 is dedicated to introduce various bearing fault types and their related vibration characteristic frequencies. The process of experimental test and its scenarios are explained in section 3. The examination and analysis of the experimental test results are presented in sections 4 and the conclusion is presented in section 5.

2. VIBRATION CHARACTERISTIC FREQUENCIES OF the BEARING FAULTS

Rolling-element bearings, which have radial loads, generate vibration even if they do not have any special defect geometrically. In fact, rolling motions in the bearing cause vibrational excitation in some frequencies [23]. However, geometrical defects, depending on their location, cause characteristic frequency components in the IM vibration. The values of the characteristic frequencies depend on the rotational frequency of the shaft as well as the geometrical parameters of the bearing, itself [2, 3]:

$$f_{IR} = \frac{f_r}{2} N_b \left(1 + \frac{D_b}{D_c} \cos \varphi\right) \quad (1)$$

$$f_{OR} = \frac{f_r}{2} N_b \left(1 - \frac{D_b}{D_c} \cos \varphi\right) \quad (2)$$

$$f_{CF} = \frac{f_r}{2} \left(1 - \frac{D_b}{D_c} \cos \varphi\right) \quad (3)$$

$$f_{BF} = \frac{D_c}{2D_b} f_r \left(1 - \left(\frac{D_b}{D_c} \cos \varphi\right)^2\right) \quad (4)$$

$$D_c = \frac{D_1 + D_2}{2} \quad (5)$$

φ is considered zero for deep groove ball bearings.

3. EXPERIMENTAL TEST SETUP AND PROCEDURE

In this section, the essential equipment for experimental tests is introduced and then the proposed research scenarios are explained. For getting laboratory test results, a 1-hp induction motor made by Motogen Co. (Tabriz, Iran) is used. Table 1 gives technical data of the IM. This IM incorporates two deep groove ball bearings with the code of 6204. In order to test with defective bearings, holes with different diameters are made on the inner race and outer race of similar bearings, and then these bearings are replaced, in turn, with the motor bearing at the drive end. Figure 2 shows two samples of such bearings. Besides, for investigation about the ball defect, a hole is created on one of the balls of another bearing as shown in Figure 3. Finally, to examine the faulty chain, the motor bearing at the drive end is replaced with a bearing in which a rupture is created on the chain as shown in Figure 4.

TABLE 1. Technical data of the induction motor

Parameter	Value	Unit
Motor Type	80-4B	---
Rated Power	1.0	Hp
Rated Voltage	220Δ/380Y	Volts
Rated Current	3.7Δ/2.15Y	A
Rated Speed	1385	Rpm
Rated Torque	5.17	Nm
Power Factor	0.76	---
Efficiency	70	%



Figure 2. Defective bearings with created holes of 2-mm diameter on the inner race and outer race



Figure 3. Defective bearing with a created hole of 2-mm diameter on a ball



Figure 4. Defective bearing with a rupture in the chain

In the first step, it is determined which axis gives a more reliable vibration signal to detect the proposed bearing defect. For this step, the vibration signal is measured on three different axes which are the X-axis, Y-axis, and Z-axis for various fault degrees. Then, in the second step, four scenarios are considered for analyzing the effectiveness of the vibration signal on the fault detection including the inner race fault with different intensities (hole diameters), the outer race fault with

different intensities, the chain fault, and the ball fault. There are three different sub-scenarios for every scenario which are focused on changes in the load level, temperature, and hole diameter size. For a comprehensive analysis, the desired IM is tested with a healthy bearing, too.

As the first sub-scenario, each state is performed at a constant temperature and a constant hole size for various loading including no-load condition, 1.5 Nm, 3 Nm, and 4.5 Nm load torques. In the second sub-scenario, each fault is tested and analyzed at a constant load as well as a constant hole size but various temperatures from 30°C to 75°C in order to evaluate the temperature effect on vibration indicators. In the final stage, the influence of the fault intensity on the vibration is evaluated by

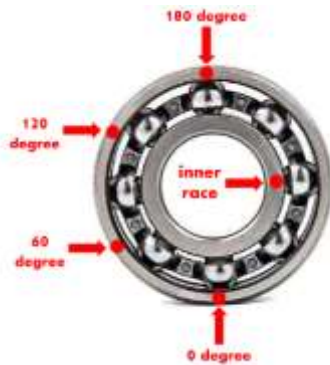


Figure 5. Fault positions on the outer race of the bearing



Figure 6. The accelerometer module installed on the motor terminal box



Figure 7. The whole experimental test setup

increasing the hole diameter from 2 mm to 5 mm at a constant temperature and a constant load.

The efficient direction for measuring vibration is considered by evaluating three different axes in the first step. Vibration signals recorded at constant temperature, constant load torque and constant hole size for various fault positions are used in this stage. The considered positions of the fault for the outer race include 0 degrees, 60 degrees, 120 degrees, and 180 degrees as shown in Figure 5. In the second step, the analysis is conducted to investigate the advantage of the vibration signal to be used for the bearing faults detection.

In the experimental tests, the temperature is measured by an infrared thermometer type GM320 of Benetech Company, and the vibration is recorded by a tri-axial accelerometer type MMA7260Q. In addition, an intermediate circuit is built to connect the mentioned sensor output to the data acquisition card PCI-1716/L of Advantech Company. The sensor module is installed horizontally on the motor terminal box with two fixing screws. The accelerometer sensor module is shown in Figure 6. For the motor variable loading, its shaft is coupled to a magnetic powder brake system. Figure 7 indicates the whole experimental test setup.

To be used in the following section, using the bearing dimensions as well as the rotor speed at different loading, the characteristic frequencies of the motor vibration is calculated according to Equations (1)-(4) and presented in Table 2 for different bearing faults.

4. TEST RESULTS ANALYSIS

In this section, the results attained through experimental tests related to different scenarios are presented and analyzed in comparison with the corresponding results attained for the healthy condition. For this purpose, the frequency spectrum analysis is performed using the Fast Fourier Transform (FFT) and the MATLAB software on the recorded vibration signals.

4. 1. Most Efficient Direction for Measuring the Vibration Signal

As mentioned previously, in the first step, the most efficient direction for the vibration measurement is determined. The experimental tests for this step are performed at constant temperature of 50°C,

TABLE 2. The characteristic frequencies of the bearing defects under different loading

Load Torque	f_{IR} (Hz)	f_{OR} (Hz)	f_{BF} (Hz)	f_{CF} (Hz)
No load	122.2	77.8	49.3	9.8
1.5 Nm	120.2	76.4	48.7	9.7
3.0 Nm	118.2	74.8	47.9	9.5
4.5 Nm	115.4	73.2	47.2	9.4

constant load of 4.5 Nm, and fixed hole diameter of 5 mm for the inner and the outer race faults as well as the healthy condition. Vibration measurements are performed in three different directions corresponding to the X-axis, Y-axis, and Z-axis (Figure 1). The sample results related to this scenario in comparison to corresponding results in the healthy condition are presented in Figures 8 to 9.

In each figure, in comparison to the spectrum related to the healthy condition, the presence of the vibration characteristic frequencies (Table 2) and their integer

multiples are evident in all the three axes of the vibration. Table 3 gives exact amplitudes of the vibration frequencies produced by the inner race fault in different directions that are presenting in Figure 8. Similarly, Table 4 presents exact amplitudes of the vibration frequencies produced by the outer race fault in different directions as shown in Figure 9.

In addition, Table 4 includes the amplitudes of the same vibration frequencies for different positions of the defect on the outer race as indicated in Figure 5. By examining Tables 3 and 4, it is observed that among the

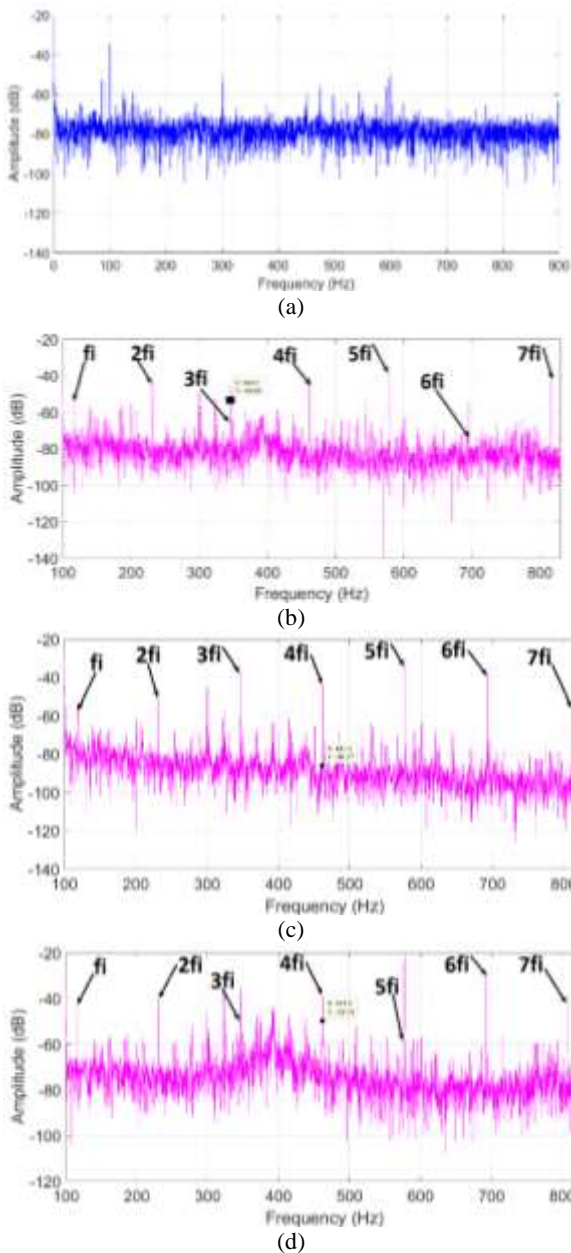


Figure 8. Motor vibration spectra under the: (a) healthy condition in Z-axis, and inner race fault condition in the: (b) X-axis, (c) Y-axis, (d) Z-axis

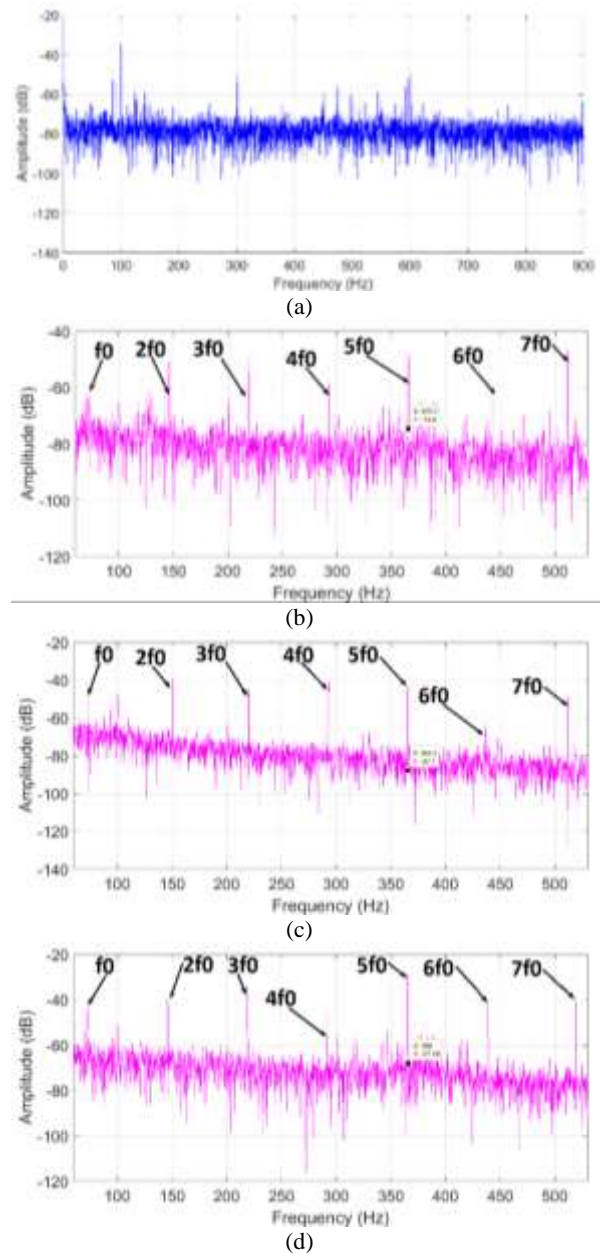


Figure 9. Motor vibration spectra under the: (a) healthy condition in Z-axis, and the outer race fault at 0 degree position in the: (b) X-axis, (c) Y-axis, (d) Z-axis

TABLE 3. Amplitudes of the vibration frequencies produced by the inner race fault (dB)

Direction	f_i	$2f_i$	$3f_i$	$4f_i$	$5f_i$	$6f_i$	$7f_i$
X-axis	-50	-43	-44	-40	-33	-53	-43
Y-axis	-54	-50	-36	-43	-30	-37	-55
Z-axis	-47	-44	-36	-42	-22	-31	-40

TABLE 4. Amplitudes of the vibration frequencies produced by the outer race fault in different position angles (dB)

Fault position	Direction	f_o	$2f_o$	$3f_o$	$4f_o$	$5f_o$	$6f_o$	$7f_o$
Zero Degree	X axis	-58	-	-	-	-	-	-
	Y axis	-48	-	-	-	-	-	-
	Z axis	-43	-	-	-	-	-	-
60 Degrees	X axis	-50	-	-	-	-	-	-
	Y axis	-47	-	-	-	-	-	-
	Z axis	-43	-	-	-	-	-	-
120 Degrees	X axis	-49	-	-	-	-	-	-
	Y axis	-33	-	-	-	-	-	-
	Z axis	-38	-	-	-	-	-	-
180 Degrees	X axis	-56	-	-	-	-	-	-
	Y axis	-48	-	-	-	-	-	-
	Z axis	-40	-	-	-	-	-	-

three axes, the fault characteristic frequency components in the Z-axis often have the highest amplitudes, and the position angle of the outer race failure has little effect on this fact.

Hence, when only the monitoring of the bearing status matters, usage of vibration sensor across all directions is not necessary and by monitoring the vibration of equipment along the Z-axis, the health or damage of the bearing can be reliably ensured. According to this result, it should be noted that all results in next subsections are measured on the Z-axis. In addition, it is observed that the fifth multiples of the characteristic frequencies ($5f_o$ and $5f_i$) have the maximum amplitude. Therefore, $5f_o$ and $5f_i$ frequencies can be harnessed for detecting the faults when the magnitudes of other related frequencies are rather low.

4. 2. Inner Race Fault

In this subsection, the experimental results related to the inner race fault are investigated. Figure 10 demonstrates the frequency spectrum of the motor vibration under the healthy condition as well as the bearing inner race fault condition at the constant temperature of 50°C, hole diameter of 2-mm and no load. The related characteristic frequency of the vibration along with its integer multiples are marked with red arrows. Each of these frequencies can be used for the inner race fault detection, so they are called the fault indicator frequencies.

The amplitudes of the frequencies in the healthy condition as well as the inner race fault of the induction motor for different loading is presented in Table 5. According to this table, apart from the $7f_{IR}$ frequency, other frequencies in the defective bearing showed a significant increase compared to their corresponding value in the healthy condition. This fact confirms their high sensitivity to the bearing defect. Table 5 also indicates that the amplitudes of the frequencies vary slightly with changing the load level; however, the loading has the lowest effect on the $5f_{IR}$ and $6f_{IR}$ frequencies.

In the second stage, the influence of temperature on the frequency amplitudes produced by the inner race fault is examined. Thus, vibration sampling is performed at of 30°C, 50°C and 75°C temperatures with constant load (1.5 Nm) and hole diameter (2 mm). The vibration frequency amplitudes attained in this stage are presented in Table 6. What stands out from this table is that the temperature changes have minimal impact on the amplitudes of the frequencies.

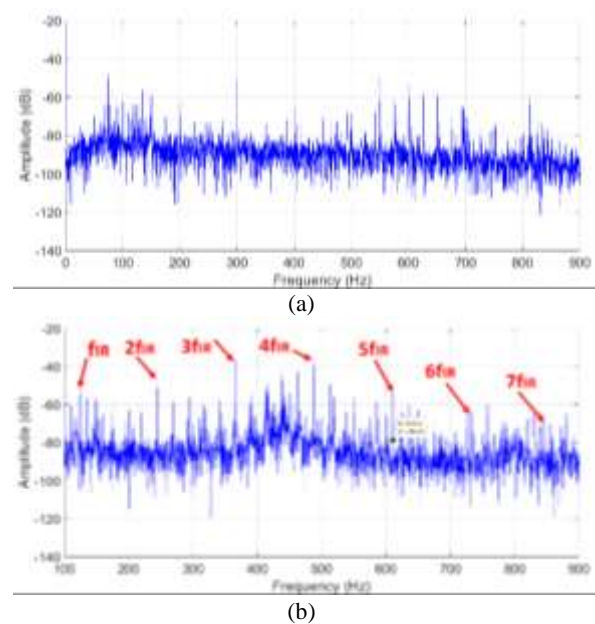


Figure 10. The vibration frequency spectra of induction motor at no load: (a) healthy condition, (b) inner race fault condition at 50°C and a hole diameter of 2-mm

In the third stage, the effect of the bearing fault severity is studied. To this end, the vibration frequencies are analyzed in the inner race fault condition with various hole diameters of 2 mm, 3 mm, 4 mm, and 5 mm at a constant load of 1.5 Nm and a constant temperature of 50°C. The results obtained for the vibration frequency amplitudes are demonstrated in Table 7. It can be seen that there is not any stable increase or decrease in amplitudes and hence they

showed fluctuation. Consequently, while the frequency amplitudes represent the bearing failure, the level of failure cannot be exactly estimated using them.

4. 3. Outer Race Fault In this subsection, the study results are presented for the outer race fault. Figure 11 illustrates the frequency spectra of the motor vibration under the outer race fault with 2 mm hole diameter, 50°C

TABLE 5. The vibration frequency amplitudes for inner race fault at the constant temperature of 50°C, fixed hole diameter of 2 mm and different load levels (dB)

Frequency component	No-load		1.5 N.m		3 N.m		4.5 N.m	
	Normal	Faulty	Normal	Faulty	Normal	Faulty	Normal	Faulty
f_{IR}	-64	-50	-62	-50	-73	-55	-74	-49
$2f_{IR}$	-77	-48	-77	-46	-75	-49	-72	-47
$3f_{IR}$	-82	-38	-82	-37	-70	-39	-72	-33
$4f_{IR}$	-84	-37	-70	-40	-73	-30	-75	-38
$5f_{IR}$	-81	-53	-74	-56	-81	-56	-70	-50
$6f_{IR}$	-76	-64	-79	-62	-72	-63	-71	-62
$7f_{IR}$	-82	-71	-87	-70	-75	-70	-74	-70

TABLE 6. The vibration frequency amplitudes for inner race fault at a constant load of 1.5 N.m, fixed hole diameter of 2mm and various temperatures (dB)

Frequency component	30° C	50° C	75° C
f_{IR}	-50	-50	-48
$2f_{IR}$	-47	-46	-47
$3f_{IR}$	-37	-37	-36
$4f_{IR}$	-36	-40	-37
$5f_{IR}$	-55	-56	-55
$6f_{IR}$	-61	-62	-61
$7f_{IR}$	-70	-70	-69

TABLE 7. The vibration frequency amplitudes of inner race fault at the constant temperature of 50°C, a constant load of 1.5 N.m and different hole diameters (dB)

Frequency component	2 mm	3 mm	4 mm	5 mm
f_{IR}	-50	-34	-40	-32
$2f_{IR}$	-46	-46	-37	-39
$3f_{IR}$	-37	-35	-29	-30
$4f_{IR}$	-40	-60	-40	-35
$5f_{IR}$	-56	-76	-57	-56
$6f_{IR}$	-62	-65	-60	-52
$7f_{IR}$	-70	-55	-57	-57

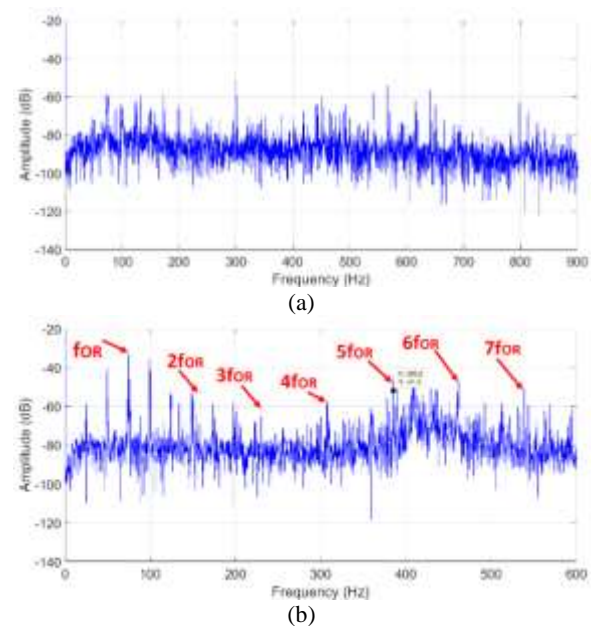


Figure 11. The vibration frequency spectra of induction motor under 1.5 Nm load torque: (a) healthy condition, (b) outer race fault condition at 50°C with 2 mm hole diameter

temperature of and 1.5 Nm load torque. The characteristic frequency f_{OR} and its integer multiples are distinguished by red arrows.

Table 8 demonstrates the frequencies amplitudes in the healthy condition as well as the outer race fault

condition under various loading. It is clear that the amplitudes of various frequencies in the outer race fault condition significantly increased in compare to the healthy condition. Moreover, the amplitudes of these frequencies are more stable than the inner race fault condition against the changes of load level especially for $2f_{OR}$ and $3f_{OR}$.

Similar to the previous subsection, the temperature influence on the amplitudes of the frequency indicators is considered. The motor vibration is sampled at a 2 mm

hole diameter, a constant load of 1.5 Nm and a variety of temperatures including 30°C, 50°C and 75°C. The results attained for the frequency amplitudes are demonstrated in Table 9. According to this table, the temperature variation has minor effect on the amplitudes.

In the last stage, the impact of the fault severity is investigated, so the experimental tests are performed at 1.5 Nm load torque, 50°C and different hole diameters of 2 mm, 3 mm, 4 mm, and 5 mm. The frequency amplitudes attained in this stage are presented in Table

TABLE 8. The vibration frequency amplitudes for outer race fault at the constant temperature of 50°C, fixed hole diameter of 2mm and different loads (dB)

Frequency component	No-load		1.5 N.m		3 N.m		4.5 N.m	
	Normal	Faulty	Normal	Faulty	Normal	Faulty	Normal	Faulty
f_{OR}	-81	-29	-57	-28	-57	-34	-54	-30
$2f_{OR}$	-75	-49	-65	-50	-64	-51	-62	-50
$3f_{OR}$	-78	-60	-73	-60	-74	-60	-72	-62
$4f_{OR}$	-81	-52	-84	-57	-60	-55	-71	-56
$5f_{OR}$	-70	-47	-70	-45	-71	-44	-71	-48
$6f_{OR}$	-73	-47	-65	-45	-71	-45	-70	-44
$7f_{OR}$	-67	-54	-73	-50	-76	-50	-69	-47

TABLE 9. The vibration frequency amplitudes of outer race fault at a constant load of 1.5 Nm, fixed hole diameter of 2-mm and various temperatures (dB)

	30° C	50° C	75° C
f_{OR}	-30	-28	-31
$2f_{OR}$	-50	-50	-51
$3f_{OR}$	-59	-60	-60
$4f_{OR}$	-54	-57	-55
$5f_{OR}$	-45	-45	-45
$6f_{OR}$	-46	-45	-45
$7f_{OR}$	-51	-50	-50

TABLE 10. The vibration frequency amplitudes of outer race fault at the constant temperature of 50°C, a constant load of 1.5 Nm and different hole diameters (dB)

	2 mm	3 mm	4 mm	5 mm
f_{OR}	-28	-25	-27	-10
$2f_{OR}$	-50	-35	-38	-28
$3f_{OR}$	-60	-47	-49	-45
$4f_{OR}$	-57	-40	-45	-55
$5f_{OR}$	-45	-33	-42	-37
$6f_{OR}$	-45	-37	-38	-31
$7f_{OR}$	-50	-42	-45	-41

10. It can be found that the amplitudes of the frequency indicators fluctuate with increasing the the fault intensity and hence there is not any uniform increase or decrease.

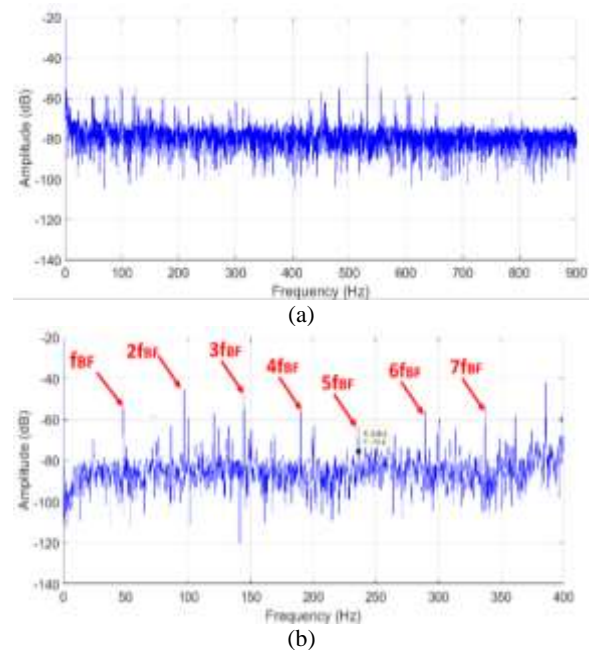


Figure 12. The vibration frequency spectra of induction motor under 3 Nm load torque: (a) healthy condition, (b) ball fault condition at 50°C with 2 mm hole diameter

Therefore, frequency indicator amplitudes may guide fault detection but the level of failure cannot be analyzed using them.

4. 4. Ball Fault In this subsection, the experimental study results for the ball fault in the bearing of the induction motor is presented. Figure 12 shows the frequency spectra of the motor vibration for the ball fault at a 2 mm hole diameter, 50°C and 3 Nm load torque. The red arrows are used to indicate the characteristic frequency f_{BF} and its integer multiples. Table 11 represents the vibration frequency amplitudes of the ball fault under various loads. According to Table 11, the amplitudes of the frequency indicators rapidly raised in compare to the healthy condition. Therefore, the indicators are useful for detecting the fault. The load variation shows a small effect on the amplitudes and it can be seen the influence is about ± 1 dB for f_{BF} and $4f_{BF}$, so, these frequencies are more stable against the load variations.

Similar to the frequency indicators of the inner race and outer race faults, the study showed that the ball fault

related frequency amplitudes have little sensitivity to the temperature variations. It should be noted that the creation of a bigger hole on the ball is so difficult due to its small size. Therefore, the experimental results regarding variation of the ball fault sesverity are not presented.

4. 5. Chain Fault The results related to the chain fault are presented in this subsection. Figure 13 shows the frequency spectra of motor vibration under the chain rupture condition at 50°C for different loads. The characteristic frequency of the chain fault along with its some integer multiples are distinguished by red arrows. However, some of the frequencies have rather small amplitudes. Table 12 gives exact amplitudes of the three strong frequencies at the healthy state and the chain fault condition. As seen, the amplitudes are increased in comparison to the healthy condition, so these frequencies can be used for the fault detection. The load changes have some impact on the frequency amplitudes but not the temperature changes.

TABLE 11. The vibration frequency amplitudes for ball fault at the constant temperature of 50°C, fixed hole diameter of 2 mm and different loads (dB)

Frequency component	No-load		1.5 N.m		3 N.m		4.5 N.m	
	Normal	Faulty	Normal	Faulty	Normal	Faulty	Normal	Faulty
f_{BF}	-70	-55	-70	-54	-59	-55	-64	-57
$2f_{BF}$	-62	-40	-64	-51	-53	-46	-54	-47
$3f_{BF}$	-58	-44	-76	-43	-74	-47	-56	-42
$4f_{BF}$	-79	-58	-66	-58	-76	-56	-66	-58
$5f_{BF}$	-78	-61	-76	-59	-70	-62	-72	-64
$6f_{BF}$	-77	-55	-85	-53	-73	-55	-70	-51
$7f_{BF}$	-85	-57	-75	-56	-76	-53	-67	-56

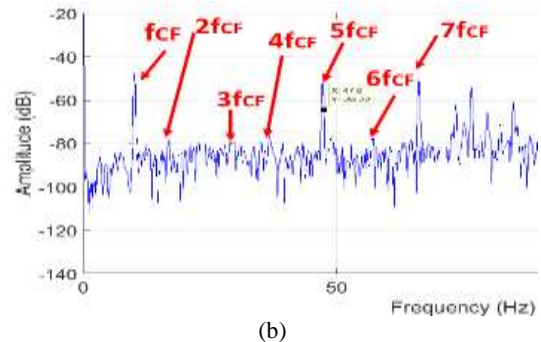
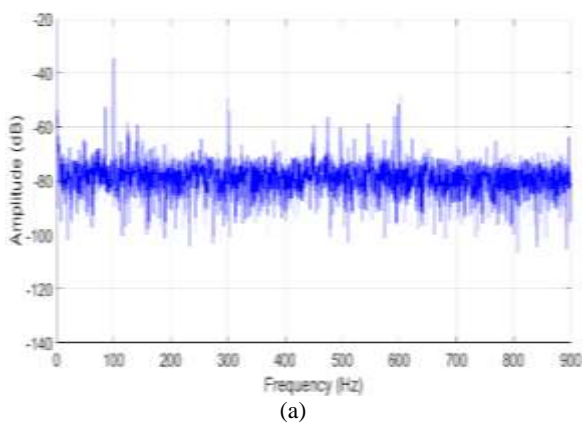


Figure 13. The vibration frequency spectra of induction motor under 4.5 Nm load torque: a) healthy condition, (b) chain fault condition at 50°C

TABLE 12. The vibration frequency amplitude for the chain fault at the constant temperature of 50°C and different loads (dB)

Frequency component	No-load		1.5 N.m		3 N.m		4.5 N.m	
	Normal	Faulty	Normal	Faulty	Normal	Faulty	Normal	Faulty
f_{CF}	-81	-58	-81	-51	-65	-49	-70	-48
$5f_{CF}$	-70	-46	-73	-44	-59	-50	-64	-52
$7f_{CF}$	-65	-45	-75	-31	-65	-41	-67	-51

5. CONCLUSION

The results attained through comprehensive experimental tests for healthy bearing as well as faulty ones demonstrate that for every bearing fault types, including the inner race fault, the outer race fault, the ball fault, and the chain fault, some specific frequencies appear in the motor vibration spectrum. These frequency indicators can be used for the fault detection. Further analysis confirms that for saving time as well as cost, vibrations amplitude can be measured only along the axis perpendicular to the motor installing surface, i.e. the Z-axis. This is because, regardless of the type and position of the fault, the related frequency amplitudes of the vibration usually have higher amplitudes along the Z-axis. In general, the temperature and load changes have minimal influence on the magnitudes of the frequency indicators. However, the amplitude of these frequencies vary with changing the fault severity.

6. REFERENCES

- Resendiz-Ochoa, E., Osornio-Rios, R. A., Benitez-Rangel, J. P., Romero-Troncoso, R. D. J. and Morales-Hernandez, L. A., "Induction Motor Failure Analysis: An Automatic Methodology Based on Infrared Imaging." *IEEE Access*, Vol. 6, (2018), 76993-77003. DOI: 10.1109/ACCESS.2018.2883988
- Saucedo-Dorantes, J. J., Miguel Delgado-Prieto, M., Ortega-Redondo, J. A., Osornio-Rios, R. A. and Romero-Troncoso, R. D. J., "Multiple-Fault Detection Methodology Based on Vibration and Current Analysis Applied to Bearings in Induction Motors and Gearboxes on the Kinematic Chain." *Shock and Vibration*, Vol. 2016, (2016), 1-13. DOI: 10.1155/2016/5467643
- Tandon, N. and Choudhury, A., "A review of vibration and acoustic measurement methods for the detection of defects in rolling element bearings." *Tribology International*, Vol. 32, No. 8, (1999), 469-480. DOI: 10.1016/S0301-679X(99)00077-8
- Chopade, S. A., Gaikwad, J. A. and Kulkarni, J. V., "Bearing fault detection using PCA and Wavelet based envelope analysis." in 2016 2nd International Conference on Applied and Theoretical Computing and Communication Technology (iCATccT), Bangalore, India, (2016). DOI: 10.1109/ICATccT.2016.7912031
- Heidari, M., "Fault Detection of Bearings Using a Rule-based Classifier Ensemble and Genetic Algorithm." *International Journal of Engineering, Transactions A: Basics*, Vol 30, No. 4, (2017), 604-609, DOI: 10.5829/idosi.ije.2017.30.04a.20
- Yuan, R., Lv, Y. and Song, G., "Fault Diagnosis of Rolling Bearing Based on a Novel Adaptive High-Order Local Projection Denoising Method." *Complexity*, Vol. 2018, (2018), 1-15, DOI: 10.1155/2018/3049318
- Mitra, S. and Koley, C., "Vibration signal analysis of induction motors used in process control operation." in 2013 IEEE 1st International Conference on Condition Assessment Techniques in Electrical Systems (CATCON). Kolkata, India, (2013). DOI: 10.1109/CATCON.2013.6737514
- Liu, J., Wu, H., and Shao, Y., "A theoretical study on vibrations of a ball bearing caused by a dent on the races." *Engineering Failure Analysis*, Vol. 83, (2018), 220-229. DOI: 10.1016/j.engfailanal.2017.10.006
- Tsytkin, M., "Induction motor condition monitoring: Vibration analysis technique — diagnosis of electromagnetic anomalies." in 2017 IEEE Autotestcon, Schaumburg, IL, USA, (2017). DOI: 10.1109/AUTEST.2017.8080483
- Attaran, B., Ghanbarzadeh, A. and Moradi, S., "A Novel Intelligent Fault Diagnosis Approach for Critical Rotating Machinery in the Time-frequency Domain." *International Journal of Engineering, Transactions A: Basics*, Vol 33, No. 4, (2020), 668-675. DOI: 10.5829/IJE.2020.33.04A.18
- Gangsar, P. and Tiwari, R., "Comparative investigation of vibration and current monitoring for prediction of mechanical and electrical faults in induction motor based on multiclass-support vector machine algorithms." *Mechanical Systems and Signal Processing*, Vol. 94, (2017), 464-481. DOI: 10.1016/j.ymsp.2017.03.016
- Kuspijani, K., Watiasih, R. and Prihastono, P. "Faults Identification of Induction Motor Based On Vibration Using Backpropagation Neural Network." in 2020 International Conference on Smart Technology and Applications (ICoSTA), Surabaya, Indonesia, (2020). DOI: 10.1109/ICoSTA48221.2020.1570615779
- Rangel-Magdaleno, J., Hayde Peregrina-Barreto, H., Ramirez-Cortes, J., Morales-Caporal, R., and Cruz-Vega, I., "Vibration Analysis of Partially Damaged Rotor Bar in Induction Motor under Different Load Condition Using DWT." *Shock and Vibration*, Vol. 5, (2016). DOI: 10.1155/2016/3530464
- Sudhakar, I., AdiNarayana, S. and AnilPrakash, M., "Condition Monitoring of a 3-Ø Induction Motor by Vibration Spectrum analysis using FFT Analyser- A Case Study." *Materials Today: Proceedings*, Vol. 4, No. 2, (2017), 1099-1105. DOI: 10.1016/j.matpr.2017.01.125
- Wissam Dehina, W., Boumehraz, M., Kratz, F. and Fantini, J., "Diagnosis and Comparison between Stator Current Analysis and Vibration Analysis of Static Eccentricity Faults in The Induction Motor." in 2019 4th International Conference on Power Electronics and their Applications (ICPEA). Elazig, Turkey, (2019). DOI: 10.1109/ICPEA1.2019.8911193
- Moiz, M. S., Shamim, S., Abdullah M., Khan, H., Hussain, I., Iftikhar, A. B. and Memon, T. D., "Health Monitoring of Three-Phase Induction Motor Using Current and Vibration Signature Analysis." in 2019 International Conference on Robotics and

- Automation in Industry (ICRAI), Rawalpindi, Pakistan, (2019). DOI: 10.1109/ICRAI47710.2019.8967356
17. Mahani, M. F. and Besanjideh, M., "Nonlinear and Non-stationary Vibration Analysis for Mechanical Fault Detection by Using EMD-FFT Method." *International Journal of Engineering, Transactions C: Aspects*, Vol. 25, No. 4, (2012), 363-372. DOI: 10.5829/idosi.ije.2012.25.04c.11
 18. Delgado-Arredondo, P. A., Morinigo-Sotelo, D., Osornio-Rios, R. A., Avina-Cervantes, J. G., Rostro-Gonzalez, H. and Romero-Troncoso, R. J., "Methodology for fault detection in induction motors via sound and vibration signals." *Mechanical Systems and Signal Processing*, Vol. 83, (2017), 568-589. DOI: 10.1016/j.ymsp.2016.06.032
 19. Novoa, C. G., Berríos, G. A. G. and Söderberg, R. A., "Predictive maintenance for motors based on vibration analysis with compact rio." in 2017 IEEE Central America and Panama Student Conference (CONESCAPAN), Panama, Panama, (2017). DOI: 10.1109/CONESCAPAN.2017.8277603
 20. Salah, M., Bacha, K. and Chaari, A., "Stator current analysis of a squirrel cage motor running under mechanical unbalance condition." in 10th International Multi-Conferences on Systems, Signals & Devices 2013 (SSD13), Hammamet, Tunisia, (2013). DOI: 10.1109/SSD.2013.6564078
 21. Marignetti, F., Rubino, G., Boukadida, Y., Conti, P., Gregorio, F., Iengo, E., Longobardi, V. G., "Noise and vibration analysis of an inverter-fed three-phase induction motor." in 2020 International Symposium on Power Electronics, Electrical Drives, Automation and Motion (SPEEDAM), Sorrento, Italy, (2020). DOI: 10.1109/SPEEDAM48782.2020.9161859
 22. Chang, S., Liu, M., Lan, C. and Hsu, W., "Lifetime Prediction for Bearings in Induction Motor." in 2019 IEEE International Conference on Industrial Cyber Physical Systems (ICPS), Taipei, Taiwan, (2019). DOI: 10.1109/ICPHYS.2019.8780366
 23. Marghitu, D. B. and Dupac, M., Machine Component Analysis with MATLAB, Butterworth-Heinemann. 2019.

Persian Abstract

چکیده

با توجه به استفاده گسترده از موتور القایی (IM) در صنایع مختلف، الزامات نظارت بر وضعیت آن به طور قابل توجهی افزایش یافته است. تشخیص عیوب موتور القایی در مدت زمان کوتاه و با دقت بالا ضروری است زیرا عدم توجه به این امر باعث خسارات مالی هنگفتی می شود. درصد بالایی از خرابی های موتور القایی ناشی از خطاهای یاتاقان است. در این مقاله، سیگنال ارتعاش برای به دست آوردن شاخص های قابل اعتماد در نظارت بر حالت های معیوب بلبرینگ موتورهای القایی به کار می رود. ابتدا جهت مناسب برای اندازه گیری ارتعاش تحلیل می شود. این تجزیه و تحلیل نشان می دهد که معمولاً مؤلفه های فرکانس ارتعاش مربوط به خطا در امتداد محور Z، یعنی محور عمود بر سطح نصب موتور، بیشترین اندازه را دارند. بنابراین، توصیه می شود سیگنال ارتعاش در محور Z اندازه گیری شود. سپس، مانیتورینگ خطای یاتاقان با سیگنال ارتعاش در سناریوهای مختلف بررسی می شود. نتایج نشان می دهد که شاخص های ارتعاش به پارامترهای محیطی مانند دما و همچنین تغییر بار موتور حساس نبوده اما شدت خطا تأثیر قابل توجهی بر روی آن ها دارد.
